Engineering Applications of Artificial Intelligence 52 (2016) 194–202

Contents lists available at ScienceDirect

Engineering Applications of Artificial Intelligence

journal homepage: www.elsevier.com/locate/engappai

ECG signal enhancement based on improved denoising auto-encoder

Peng Xiong [a], Hongrui Wang [a,b], Ming Liu [b], Suiping Zhou [c], Zengguang Hou [d], Xiuling Liu [b,*]

[a] College of Electronic and Information Engineering, Yanshan University, Qinhuangdao, China
[b] Key Laboratory of Digital Medical Engineering of Hebei Province, College of Electronic and Information Engineering, Hebei University, Baoding, China
[c] School of Science and Technology, Middlesex University, UK
[d] Institute of Automation, Chinese Academy of Sciences, Beijing, China

ARTICLE INFO

Article history:
Received 2 October 2015
Received in revised form
6 February 2016
Accepted 27 February 2016

Keywords:
Denoising auto-encoder (DAE)
ECG signal denoising
Wavelet transform (WT)
Deep neural network (DNN)

ABSTRACT

The electrocardiogram (ECG) is a primary diagnostic tool for examining cardiac tissue and structures. ECG signals are often contaminated by noise, which can manifest with similar morphologies as an ECG waveform in the frequency domain. In this paper, a novel deep neural network (DNN) is proposed to solve the above mentioned problem. This DNN is created from an improved denoising auto-encoder (DAE) reformed by a wavelet transform (WT) method. A WT with scale-adaptive thresholding method is used to filter most of the noise. A DNN based on improved DAE is then used to remove any residual noise, which is often complex with an unknown distribution in the frequency domain. The proposed method was evaluated on ECG signals from the MIT-BIH Arrhythmia database, and added noise signals were obtained from the MIT-BIH Noise Stress Test database. The results show that the average of output signal-to-noise ratio (SNR) is from 21.56 dB to 22.96 dB, and the average of root mean square error (RMSE) is less than 0.037. The proposed method showed significant improvement in SNR and RMSE compared with the individual processing with either a WT or DAE, thus providing promising approaches for ECG signal enhancement.

1. Introduction

Cardiovascular disease is one of the most common threats to human health and is characterized by a high disease incidence, disability rate, and mortality. Development of telemedicine now allows for remote electrocardiogram (ECG) monitoring and provides information for the diagnosis and treatment of cardiovascular diseases. Specifically, remote ECG monitoring systems can improve early diagnosis accuracy of coronary disease states. Telemedicine practices have recently expanded to include qualitative and quantitative analysis of arrhythmia and evaluation of restenosis in patients who have suffered a myocardial infarction.

The ECG signal from remote ECG monitoring systems provides an effective method for detecting heart diseases. The ECG signal is measured by surface electrodes placed on the skin of patients. However, the signal is often corrupted by large amounts of noise from muscle artifacts (MA), electrode motion (EM), and baseline wander (BW). These noise signals may be confused with the ectopic ECG signals (Rahman et al., 2011). Hence, noisy ECG signals should be enhanced by removing the noise components for further processing such as feature extraction and pattern recognition.

Many researchers have reported on different techniques for denoising ECG signals such as empirical mode decomposition (EMD) (Karagiannis and Constantinou, 2011; Kabir and Shahnaz, 2012), adaptive filtering (Sajjad et al., 2012; Rahman et al., 2012; Moradi et al., 2014), and the wavelet method (Awal et al., 2012, 2014; KapilTajane and Pitale, 2014; Reddy et al., 2009; Gokhale, 2012; Smital et al., 2013).

Karagiannis and Constantinou (2011) studied the performance of EMD on ECG signals. Noisy ECG signals were processed with EMD in order to extract the intrinsic mode functions (IMFs). The algorithm implemented by Karagiannis deduced a 95% bound for the white Gaussian noise in an ECG time series. Kabir and Shahnaz (2012) proposed a windowing method in conjunction with EMD in order to reduce the noise from the initial IMFs while preserving the QRS complex and yielding a relatively clean ECG signal. However, it is known that the Hilbert transform intrinsic to EMD cannot separate similar frequency signals. Therefore, this method of noise reduction may filter out P-waves and T-waves from the signal, potentially resulting in misdiagnosis.

Rahman et al. (2012) proposed several adaptive recurrent filters for remote ECG signal denoising, such as a signed regressor algorithm, a normalized least mean square (LMS) and an error nonlinear signed regressor LMS. Simulation results from Rahman confirmed that the performance of sign-based algorithms is better than the LMS method. However, adaptive filters often require a

* Corresponding author.
E-mail address: liuxiuling121@hotmail.com (X. Liu).

http://dx.doi.org/10.1016/j.engappai.2016.02.015
0952-1976/

noise reference signal which is difficult to obtain from a typical ECG signal acquisition system.

Wavelet transform (WT) based techniques are more popular and widely implemented because of their ability to characterize the time-frequency domain information of a time-domain signal (KapilTajane and Pitale, 2014). Gokhale (2012) used a WT method to remove power line interference from ECG signals. Smital used an adaptive wavelet Wiener filtering method for denoising broad band electromyography from ECG signals. In the work of Smital et al. (2013), the dyadic stationary wavelet transform in the Wiener filter was used to estimate the noise-free signal. Then, a suitable filter bank and additional parameters of the Wiener filter with respect to the signal-to-noise ratio (SNR) were obtained. The adaptive characteristics of the Wiener filtering method allowed for improved performance. However, noise can manifest with similar morphologies as an ECG waveform in the frequency domain. Often, the frequency spectrum of this noise may completely overlap with the ECG signal (Clifford et al., 2006), specifically with the ST segment and BW, and/or the QRS wave group and motion artifacts (Sameni et al., 2007). WT processing could filter most of the noise, which is separated from an ECG signal to some degree after wavelet decomposition (Reddy et al., 2009). However, the residual noise, whose characteristics are complex and distribution is unknown in the frequency domain, is difficult to filter by conventional methods. Therefore, the main disadvantage of WT methods is the inability to perform signal analysis independent of the frequency domain.

Based on the above analysis, it is clear that existing methods cannot meet the ECG noise reduction requirements needed for remote analysis. Long-term monitoring of cardiac patients and extensive telemedicine data provide a large database of ECG studies and serves as a good platform for ECG intelligent analysis. The depth model, which learns features based on a large database, performs better than the shallow model which relies on characterizing the inherent data rich information. Recently, deep neural network (DNN) models, such as the stacked denoising autoencoder (DAE), constructed with a series of DAEs (Vincent et al., 2008; Vincent, 2011), or the deep belief network formed by a series of restricted Boltzmann machines (RBM) (Rodrigues and Couto, 2012), have been widely used in the area of signal denoising and feature learning (Swietojanski et al., 2014; Erhan et al., 2014; Dahl et al., 2012). Rodrigues and Couto (2012) introduced an ECG denoising method based on RBM with three hidden layers, resulting in improved ECG denoising due to EM artifact noise.

This study proposes an improved method for denoising ECG signals using a DNN created from an improved DAE reformed by a WT method, taking advantage of the available big data platform. The architecture and calculation of the improved DAE by WT with soft thresholding are presented. A DNN created from the proposed method for denoising is established. Experimental results show that the proposed method outperforms both the WT and DAE individually.

2. Materials and methods

2.1. The overall structure

The objective of the proposed algorithm is to achieve enhanced ECG signals by removing the basic and residual noise components via and improved DAE with WT. A block diagram of the proposed deep learning method, which includes the establishment of a DNN and the ECG signal denoising is illustrated in Fig. 1.

The DNN is based on the improved DAE. While the training for the DNN, the clean input signal is corrupted by adding noise with the encoder of DAE. Then, the signal is denoised by the WT with adaptive thresholding. After that, the signal is used to reconstruct the original input with the decoder of DAE.

For ECG signal enhancement, a noisy ECG signal would be denoised through the WT with adaptive thresholding first and then denoised with the DNN established previously.

2.2. ECG database

Experiments in this study used ECG signals from the MIT-BIH Arrhythmia Database (Moody and Mark, 2001) for performance analysis. The ECG signals in the database include 48 Holter recordings, all slightly over 30 min long, obtained by the Beth Israel Hospital Arrhythmia Laboratory. Each recording included signals from two leads: the modified limb lead II and the modified lead V1. Occasionally, the second signal was from lead V2 or V5. This configuration is routinely used by the BIH Arrhythmia Laboratory. Experiments in this study used the limb lead II signal, which has a sampling frequency of 360 Hz.

The noise signals selected for use in this study were from the MIT-BIH Noise stress database, which included 3 half-hour recordings of noise typical in ambulatory ECG recordings (Moody et al., 1984). Specially, the noise signals for MA, EM, and BW, which were obtained from physically active volunteers, were added to the ambulatory ECG recordings with a set SNR to obtain a noisy ECG signal.

2.3. The proposed method

2.3.1. WT with soft threshold

The Daubechies 6 (DB 6) was chosen as the base wavelet. Wavelet coefficients d_j were then obtained for each scale after an eight-layer wavelet decomposition to obtain a clean ECG signal. A scale adaptive thresholding method was used in this work in order to ensure maximum noise removal while retaining as much of the useful signal as possible (Reddy et al., 2009):

$$T_j = \frac{\sigma_j \sqrt{2\ln(n)}}{e^{j-1}} \tag{1}$$

where T_j is the set threshold, $j \in U = \{1,2,3,4,5,6,7,8\}$ is the layer number of the wavelet decomposition, n is the number of samples, and σ_j is the mean absolute value of wavelet coefficients: $\sigma_j = \frac{median|d_j|}{0.6745}$. The wavelet coefficients d_j were then processed by the soft threshold method:

$$\hat{d}_j^i = \begin{cases} \mathrm{sgn}(d_j^i)(|d_j^i| - T_j), & |d_j^i| \geq T_j \\ 0, & |d_j^i| \leq T_j \end{cases} \tag{2}$$

where $j = 1,2,3,4,5,6,7,8$ is the layer number of the wavelet decomposition, and $i = 1,2,\ldots,n$ is the number of samples. The initial denoised ECG signals a were obtained by reconstructing the wavelet coefficients with Eq. (3) after the soft threshold processing:

$$a = \sum_{j \in D} (\hat{d}_j) \tag{3}$$

where $D \in U$ is selected according to the frequency distribution of the ECG signal (Vullings et al., 2011).

2.3.2. The DNN based on the improved DAE

An appropriate neighborhood was selected according to the periodic nature of ECG signals and the sampling frequency. For the sampling point a_i of the initial denoised ECG signal, the neighborhood $V(a_i, \delta) = \{x | a_i - \delta \leq x \leq a_i + \delta\}$ was used as one sample for training and testing the DNN.

In order to denoise the ECG signals, the number of output notes must be the same as the number of input notes and is equal to the

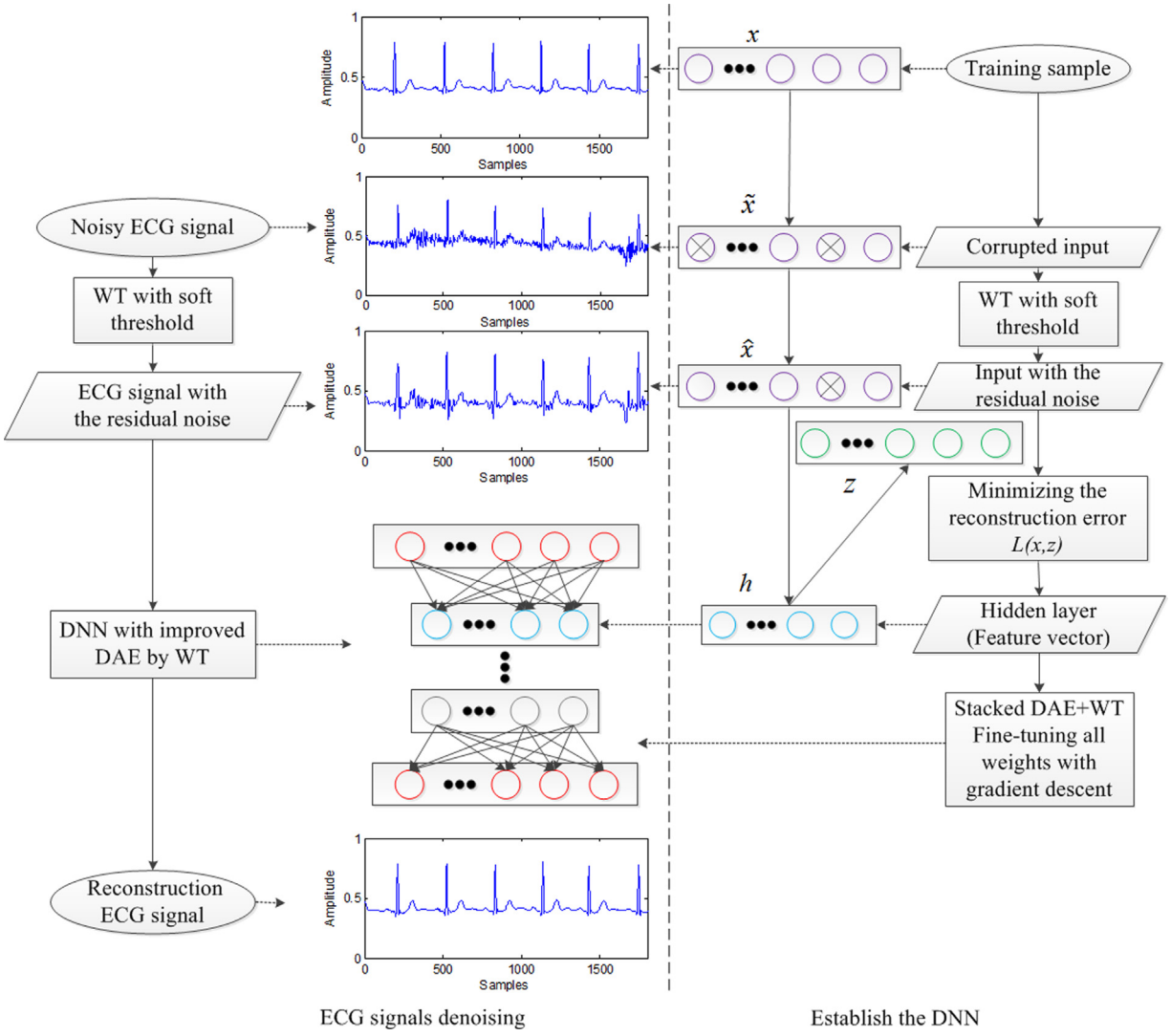

Fig. 1. Block diagram of the proposed deep learning method.

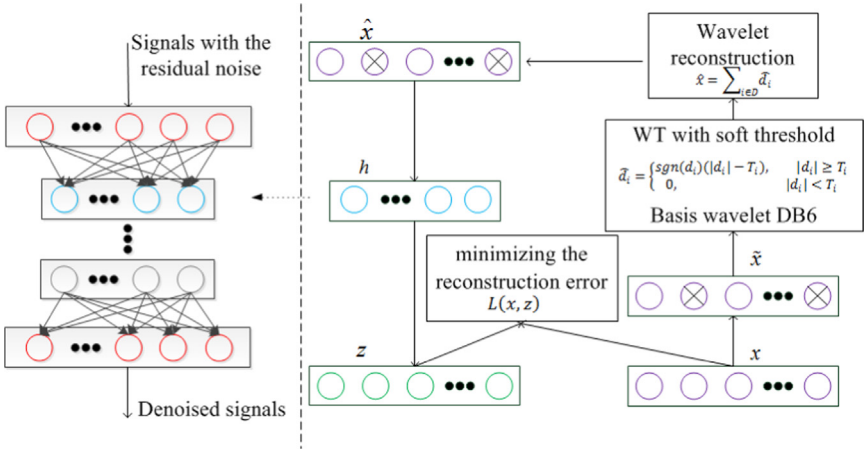

Fig. 2. The DNN is based on the improved DAE.

length of the sample vector $v = V(a_i, \delta)$. Based on experience, the number of notes of the hidden layers must be half that of the input. The sample vector v was mapped to $x \in [0,1]^p$ as the input of the improved DAE by min–max normalization. The architecture of the improved DAE is shown in the right part of Fig. 2.

The input $x \in [0,1]^p$ used for DAE training was initially corrupted by means of a stochastic mapping $\tilde{x} \sim q(\tilde{x}|x)$. Then, $\tilde{x}$ was denoised by WT with soft thresholding as mentioned above. The wavelet coefficients d_j on each scale were then obtained after eight-layer wavelet decomposition from $\tilde{x}$. Next, $\hat{x}$ was found with

Eq. (3), $\hat{x} = \sum_{j \in D}(\hat{d}_j)$. Following this, $\hat{d}_j$ was processed by Eq. (2) with the wavelet coefficient d_j.

After that, a feature vector $h = f_\theta(\hat{x}) = s(W\hat{x} + b)$ was computed from the vector $\hat{x}$, where $\theta = \{W, b\}$ are parameters for the encoder of the DAE, and $s(x) = 1/(1+e^{-x})$ is a Sigmoid function.

A reconstruction vector $z = g_{\theta'}(h) = s(W'h + b')$, where $\theta' = \{W', b'\}$ are parameters with weight matrix $W' = W^T$, was produced by mapping from feature space back to input space. This vector is the decoder of the DAE.

For each sample $v^{(i)}$ is mapped to $x^{(i)}$, corrupted to $\tilde{x}^{(i)}$, denoised to $\hat{x}^{(i)}$, mapped to the hidden vector $h^{(i)}$, and finally reconstructed as $z^{(i)}$. The parameters are optimized by minimizing the reconstruction error:

$$\theta^*, \theta'^* = \arg\min_{\theta,\theta'} \frac{1}{n}\sum_{i=1}^{n} L(x^{(i)}, z^{(i)}) = \frac{1}{n}\sum_{i=1}^{n} L\left\{x^{(i)}, g_{\theta'}[f_\theta(\hat{x}^{(i)})]\right\} \quad (4)$$

where n is the number of training samples, L is loss function with the distance of Bernoulli. The distance is measured with cross-entropy:

$$L(x, z) = -\sum_{k=1}^{p}(x_k \log z_k + (1-x_k)\log(1-z_k)) \quad (5)$$

The improved DAE is trained with a gradient descent to minimize the loss function and find the optimal parameters. When the value of the loss function is small enough, the output of the improved DAE $z^{(i)}$ is thought to replace the clean signal $x^{(i)}$. The DNN is established with 2 hidden layers using the DAE for ECG signal denoising (the left part of Fig. 2). According to the periodic nature of ECG signals and the sampling frequency of the MIT-BIH Arrhythmia and MIT-BIH Noise Stress Test databases, the neighborhood radius was found to be $\delta = 50$. Therefore, the methods described employ a DNN structured as 101-50-50-101.

2.3.3. Training and application of the DNN

In order to compare the proposed method with the literature (Samit et al., 2013), the WT with soft threshold (Reddy et al., 2009), the Back Propagation neural network (BPNN) (Moody and Mark, 2001) and the stacked DAE (Vincent et al., 2008), the same 10 recordings of ECG signals from the MIT-BIH Arrhythmia database (Moody et al., 1984) were used for performance analysis. Noise signals were again selected from the MIT-BIH Noise Stress Test database (Xiaopeng and Chen, 2014). MA, EM, and BW noise signals were added to the ECG signal with SNRs of 0 dB, 1.25 dB, and 5 dB, respectively.

The established DNN is trained by gradient descent layer by layer, beginning with the lowest layer DAE. The lowest layer feature extraction from a clean ECG signal x is $h_1 = f_{\theta^0}(\hat{x})$. The second layer feature extraction of h_1 is $h_2 = f_{\theta^1}(\hat{h_1})$. The second layer processing updates the weights and does not affect the underlying layer. The weight of the improved DAE is initialized layer by layer, in addition to fine-tuning all the weights with a gradient descent algorithm.

After training the DNN, the noisy ECG signals were sent through the WT with soft threshold, and then into the established DNN to obtain the denoised signals. However, multiple noise signals remained even after noise reduction for the same sample point between different reconstructed data from the deep architectures. Calculating the mean of the overlapping portions allows for the normalization of denoised ECG signal data and fusion after excluding negligent errors. In this study, this procedure was repeated ten times. Each time, the training data contained 30 000 samples and the testing data contained 2000 samples. The results in the tables are the average of all 10 trials.

3. Results and discussion

3.1. Performance indicators

The performance of the proposed method was evaluated based on the calculated SNR and RMSE. If $x(n)$ is the original ECG signal, $x_m(n)$ represents the denoised ECG signal and RMSE is defined as:

$$RMSE = \sqrt{\frac{1}{N}\sum_{n=0}^{N-1}[x(n) - x_m(n)]^2} \quad (6)$$

and SNR defied as:

$$SNR = 10\log\frac{\sum_{n=0}^{N-1}[x(n)]^2}{\sum_{n=0}^{N-1}[x_m(n) - x(n)]^2} \quad (7)$$

3.2. Experimental results for noise contaminated signals

Ten recordings of ECG signals from the MIT-BIH Arrhythmia Database were used for performance analysis in order to compare with the results of the other method in literatures. Additionally, the typical noises in ambulatory ECG recordings including BW, MA and EM, were individually selected from the MIT-BIH Noise stress database and added to the ten recordings for analysis. The proposed method was compared with the Stockwell transform (S-Transform) (Samit et al., 2013), improved thresholding based on WT (Reddy et al., 2009), Back Propagation neural network (BPNN) (Xiaopeng and Chen, 2014) and stacked DAE (Vincent et al., 2008) methods for each ECG signal.

Fig. 3 shows the experimental results of removing the BW noise from an ECG signal. Fig. 3a represents the original ECG signal (MIT-

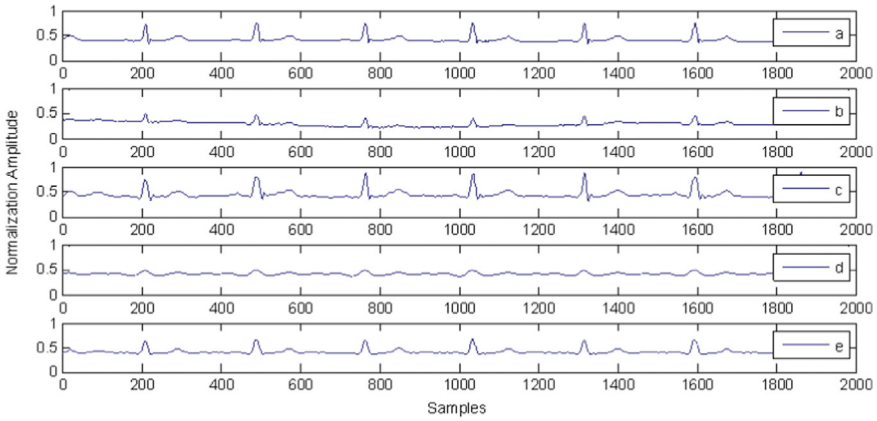

Fig. 3. Experimental result of the BW noise case.

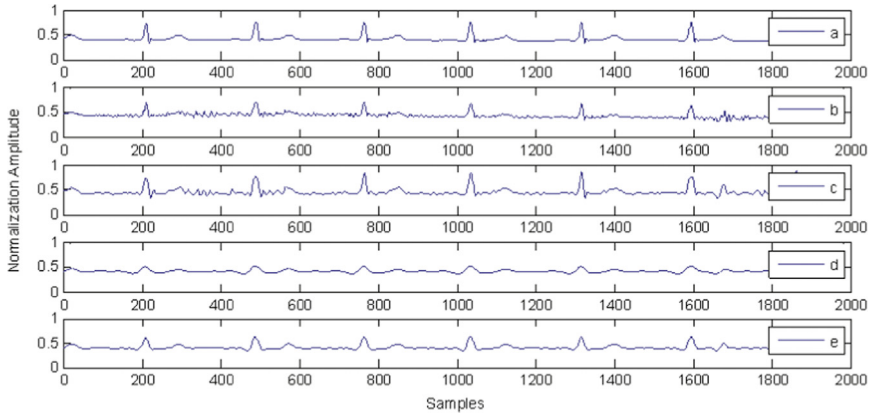

Fig. 4. Experimental result of the MA noise case.

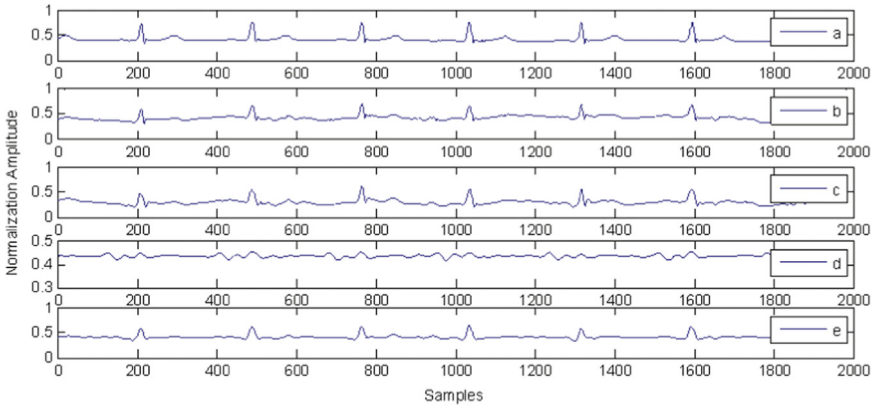

Fig. 5. Experimental result of the EM noise case.

Table 1
Experimental results for BW noise.

MIT-BIH recording number			103	105	111	116	122	205	213	219	223	230	Average
S-Transform method	0 dB	*SNR*	11.4	11.56	9.22	9.01	10.58	9.31	11.57	11.55	12.14	11.68	10.80
		RMSE	0.269	0.264	0.346	0.354	0.296	0.342	0.264	0.265	0.247	0.261	0.291
	1.25 dB	*SNR*	12.06	12.23	9.61	9.35	11.17	9.7	12.22	12.22	12.95	12.35	11.39
		RMSE	0.249	0.245	0.331	0.341	0.276	0.327	0.245	0.245	0.225	0.241	0.273
	5 dB	*SNR*	13.54	13.77	10.41	10.04	12.38	10.46	13.77	13.65	14.81	13.89	12.67
		RMSE	0.210	0.205	0.302	0.315	0.240	0.300	0.205	0.208	0.182	0.202	0.237
WT method	0 dB	*SNR*	14.87	31.53	18.41	20.00	9.12	22.64	20.83	18.69	17.34	22.23	19.57
		RMSE	0.074	0.014	0.060	0.042	0.138	0.037	0.034	0.040	0.063	0.041	0.054
	1.25 dB	*SNR*	14.88	31.91	18.42	20.06	8.54	22.73	20.47	20.22	17.40	22.22	19.69
		RMSE	0.074	0.013	0.060	0.042	0.147	0.037	0.036	0.034	0.063	0.041	0.055
	5 dB	*SNR*	14.90	32.71	18.43	20.10	8.22	22.91	19.11	21.44	17.51	22.18	19.75
		RMSE	0.074	0.012	0.060	0.041	0.153	0.036	0.042	0.029	0.062	0.041	0.055
BPNN method	0 dB	*SNR*	9.27	9.28	4.84	12.32	15.75	14.59	11.62	11.92	13.18	7.46	11.02
		RMSE	0.130	0.130	0.178	0.252	0.151	0.073	0.178	0.191	0.153	0.128	0.156
	1.25 dB	*SNR*	11.44	9.54	6.87	12.67	16.34	14.83	12.37	12.88	13.52	8.69	11.92
		RMSE	0.105	0.126	0.142	0.244	0.143	0.072	0.164	0.171	0.145	0.116	0.143
	5 dB	*SNR*	12.55	9.67	8.23	13.38	16.87	15.86	13.34	13.63	15.34	9.42	12.83
		RMSE	0.099	0.122	0.118	0.224	0.134	0.063	0.145	0.155	0.115	0.106	0.128
DAE method	0 dB	*SNR*	20.38	24.90	23.04	18.84	19.48	20.08	19.92	19.30	22.94	20.53	20.94
		RMSE	0.038	0.029	0.035	0.047	0.040	0.050	0.036	0.037	0.031	0.049	0.039
	1.25 dB	*SNR*	20.55	23.27	23.07	19.53	19.90	20.12	20.32	19.83	23.74	20.67	21.30
		RMSE	0.038	0.028	0.035	0.043	0.038	0.049	0.035	0.035	0.029	0.048	0.038
	5 dB	*SNR*	20.77	25.47	23.03	21.60	21.00	20.30	21.34	21.15	25.41	21.03	22.11
		RMSE	0.037	0.027	0.035	0.034	0.034	0.048	0.031	0.030	0.024	0.046	0.035
Proposed method	0 dB	*SNR*	23.78	25.40	23.31	23.51	20.07	20.07	21.30	23.02	24.25	22.72	22.74
		RMSE	0.026	0.028	0.034	0.027	0.050	0.050	0.032	0.024	0.027	0.037	0.034
	1.25 dB	*SNR*	23.82	25.42	23.32	23.59	20.08	20.08	21.36	23.31	24.41	22.74	22.81
		RMSE	0.026	0.028	0.034	0.027	0.050	0.050	0.032	0.023	0.027	0.037	0.033
	5 dB	*SNR*	23.89	25.45	23.35	23.76	20.08	20.08	21.46	24.08	24.64	22.79	22.96
		RMSE	0.025	0.027	0.034	0.026	0.050	0.050	0.031	0.021	0.026	0.037	0.033

BIH recording no.116) and Fig. 3b demonstrates the noisy ECG signal with BW noise added in with a SNR of 1.25 dB. Fig. 3c shows the denoised result using the WT method, and Fig. 3d and e show the denoised results with the DAE method and the proposed method, respectively. Fig. 3d was the least effective in denoising, though the differences between Fig. 3c and e are small.

Fig. 4 shows the experimental results of removing the MA noise from an ECG signal. Fig. 4a represents the original ECG signal (MIT-BIH recording no.116), and Fig. 4b demonstrates the noisy ECG signal with MA noise added with a SNR of 1.25 dB. Fig. 4c shows the denoised results using the WT method and includes noise with morphology similar to a P-wave and a T-wave. In Fig. 4d, the denoised result obtained with the DAE method is shown and the QRS wave group is almost distorted. The results shown in Fig. 4e were obtained with the proposed method and demonstrate an improvement over the results of Fig. 4c and d.

Fig. 5 shows the experimental results of removing the EM noise from an ECG signal. Fig. 5a represents the original ECG signal (MIT-BIH recording no.116) and Fig. 5b demonstrates the noisy ECG signal with EM noise added in with a SNR of 1.25 dB. Fig. 5c shows the denoised results using WT method and includes noise with morphology similar to a P-wave and a T-wave. In Fig. 5d, the denoised result obtained with the DAE method is shown and the QRS wave group is seriously distorted. The results shown in Fig. 5e were obtained with the proposed method and demonstrate an improvement over the results of Fig. 5c and d.

Table 1 illustrates the RMSE and SNR of the BW noise-enhanced signals using the S-Transform, improved WT, BPNN, DAE and the proposed method. The SNR for each recording after denoising for the BW noise case are shown in Fig. 6. The S-Transform, BPNN and the WT methods provided minor improvement in the RMSE and SNR, and the DAE method provided further enhancement. The proposed method showed further improvement over the DAE method. For example, the results for recording number 223 showed that for a 1.25 dB input SNR, the S-Transform, WT, BPNN, and DAE outputs had a SNR of 12.95 dB, 17.40 dB, 13.52 dB, and

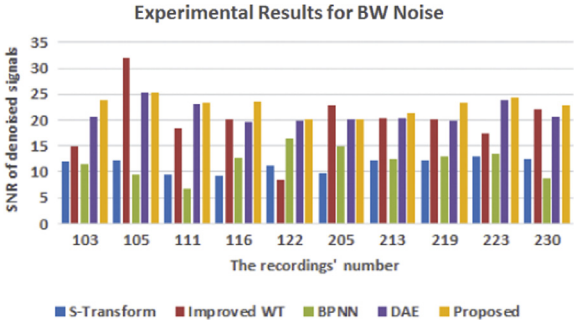

Fig. 6. De-noised SNR for the BW noise case with 1.25 dB.

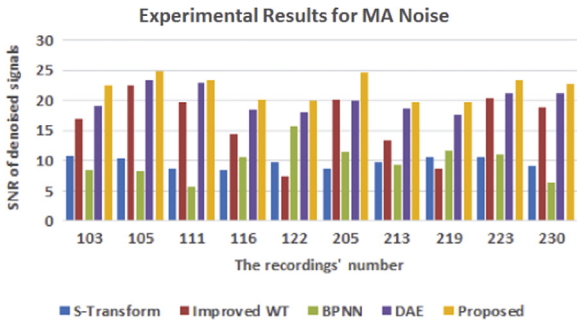

Fig. 7. De-noised SNR for the MA noise case with 1.25 dB.

Table 2
Experimental results for MA noise.

MIT-BIH recording number			103	105	111	116	122	205	213	219	223	230	Average
S-transform method	0 dB	*SNR*	10.41	10.02	8.21	8.19	9.20	8.32	8.79	10.05	9.95	8.70	9.18
		RMSE	0.302	0.316	0.389	0.389	0.347	0.384	0.363	0.314	0.318	0.367	0.349
	1.25 dB	*SNR*	10.89	10.42	8.66	8.51	9.67	8.61	9.67	10.61	10.56	9.01	9.66
		RMSE	0.286	0.301	0.369	0.375	0.328	0.371	0.329	0.295	0.297	0.355	0.331
	5 dB	*SNR*	12.63	12.76	9.94	9.75	11.69	9.91	12.53	12.89	13.44	10.15	11.57
		RMSE	0.234	0.230	0.318	0.325	0.260	0.320	0.236	0.227	0.213	0.311	0.267
WT method	0 dB	*SNR*	19.66	22.09	20.02	12.44	6.71	21.23	11.83	7.33	18.58	18.03	15.79
		RMSE	0.044	0.040	0.050	0.100	0.182	0.044	0.096	0.149	0.055	0.066	0.083
	1.25 dB	*SNR*	16.87	22.49	19.69	14.40	7.43	20.24	13.27	8.68	20.32	18.86	16.23
		RMSE	0.060	0.039	0.052	0.080	0.167	0.049	0.081	0.127	0.045	0.060	0.076
	5 dB	*SNR*	15.79	24.11	18.81	19.15	11.14	16.51	18.94	14.55	21.41	21.14	18.16
		RMSE	0.067	0.032	0.057	0.046	0.109	0.075	0.042	0.065	0.040	0.046	0.058
BPNN method	0 dB	*SNR*	6.84	7.83	5.59	10.04	15.34	10.32	9.17	11.11	10.49	6.19	9.29
		RMSE	0.166	0.153	0.162	0.326	0.153	0.120	0.237	0.209	0.171	0.155	0.185
	1.25 dB	*SNR*	8.55	8.30	5.64	10.60	15.69	11.42	9.31	11.60	11.02	6.44	9.86
		RMSE	0.147	0.145	0.161	0.309	0.151	0.107	0.234	0.198	0.183	0.149	0.178
	5 dB	*SNR*	10.21	8.39	5.76	11.65	16.14	12.96	10.84	13.63	12.86	8.46	11.09
		RMSE	0.122	0.143	0.157	0.268	0.145	0.089	0.197	0.157	0.158	0.119	0.156
DAE method	0 dB	*SNR*	18.92	22.97	22.90	17.92	17.96	20.03	18.18	16.18	20.29	21.11	19.65
		RMSE	0.046	0.036	0.036	0.053	0.047	0.050	0.044	0.049	0.043	0.046	0.045
	1.25 dB	*SNR*	19.07	23.30	22.88	18.48	18.09	20.03	18.70	17.66	21.21	21.22	20.06
		RMSE	0.045	0.035	0.036	0.049	0.042	0.050	0.041	0.044	0.039	0.045	0.043
	5 dB	*SNR*	19.31	24.12	22.95	20.61	21.73	20.14	20.15	20.05	23.69	21.33	21.41
		RMSE	0.044	0.032	0.035	0.038	0.031	0.050	0.036	0.033	0.029	0.044	0.037
Proposed method	0 dB	*SNR*	21.38	24.72	23.15	19.22	19.57	24.23	19.59	18.80	22.91	22.58	21.62
		RMSE	0.034	0.030	0.035	0.045	0.040	0.031	0.038	0.039	0.032	0.038	0.036
	1.25 dB	*SNR*	22.41	24.86	23.27	20.22	20.02	24.49	19.78	19.63	23.41	22.60	22.07
		RMSE	0.031	0.029	0.034	0.040	0.038	0.030	0.037	0.034	0.030	0.038	0.034
	5 dB	*SNR*	23.33	25.13	23.33	22.41	20.63	24.67	20.63	21.97	24.21	22.63	22.89
		RMSE	0.027	0.028	0.034	0.031	0.036	0.030	0.034	0.027	0.028	0.038	0.031

Table 3
Experimental results for EM noise.

MIT-BIH recording number			103	105	111	116	122	205	213	219	223	230	Average
S-transform method	0 dB	*SNR*	6.41	6.13	5.45	5.47	5.87	5.59	5.85	6.05	6.21	6.29	5.93
		RMSE	0.478	0.493	0.534	0.533	0.509	0.525	0.510	0.498	0.489	0.484	0.505
	1.25 dB	*SNR*	7.47	7.35	6.40	6.32	6.96	6.47	7.06	7.17	7.45	7.48	7.01
		RMSE	0.423	0.429	0.478	0.483	0.449	0.475	0.444	0.438	0.424	0.423	0.447
	5 dB	*SNR*	10.32	10.40	8.54	8.32	9.60	8.55	10.12	10.04	10.74	10.45	9.71
		RMSE	0.305	0.302	0.374	0.384	0.331	0.374	0.312	0.315	0.290	0.300	0.329
WT method	0 dB	*SNR*	9.51	21.47	9.34	9.63	9.71	18.29	15.02	13.15	18.11	11.99	13.62
		RMSE	0.138	0.044	0.171	0.138	0.128	0.063	0.067	0.076	0.058	0.132	0.102
	1.25 dB	*SNR*	10.37	23.08	9.65	10.56	9.51	20.30	15.80	13.85	21.10	12.93	14.72
		RMSE	0.125	0.037	0.165	0.124	0.132	0.050	0.061	0.070	0.040	0.119	0.092
	5 dB	*SNR*	13.07	28.37	14.96	13.77	8.65	21.36	19.20	16.20	24.05	15.91	17.55
		RMSE	0.091	0.020	0.090	0.086	0.145	0.043	0.040	0.054	0.029	0.084	0.068
BPNN method	0 dB	*SNR*	8.83	7.49	4.69	9.49	14.39	11.84	10.38	11.19	10.48	6.17	9.50
		RMSE	0.139	0.160	0.181	0.347	0.178	0.099	0.208	0.209	0.203	0.151	0.188
	1.25 dB	*SNR*	9.17	7.55	5.56	10.58	14.70	12.18	10.77	11.99	12.36	7.54	10.24
		RMSE	0.128	0.157	0.166	0.306	0.168	0.097	0.197	0.192	0.167	0.131	0.171
	5 dB	*SNR*	11.22	8.08	7.91	11.09	14.49	13.19	12.38	12.07	13.77	8.67	11.29
		RMSE	0.108	0.135	0.125	0.281	0.139	0.087	0.162	0.182	0.139	0.114	0.147
DAE method	0 dB	*SNR*	18.94	23.45	22.33	19.18	17.87	20.08	19.20	17.53	22.66	20.79	20.20
		RMSE	0.047	0.035	0.038	0.046	0.047	0.050	0.039	0.045	0.033	0.048	0.043
	1.25 dB	*SNR*	19.07	23.82	22.43	19.69	18.98	20.11	19.74	18.32	23.20	20.91	20.63
		RMSE	0.046	0.033	0.038	0.043	0.042	0.049	0.037	0.041	0.031	0.047	0.041
	5 dB	*SNR*	19.30	24.56	22.66	21.00	21.16	20.24	20.98	20.08	24.39	21.40	21.58
		RMSE	0.041	0.030	0.037	0.037	0.033	0.049	0.033	0.034	0.027	0.044	0.037
Proposed method	0 dB	*SNR*	22.75	23.70	23.39	21.34	17.70	23.47	19.33	18.38	23.17	22.40	21.56
		RMSE	0.029	0.033	0.034	0.035	0.050	0.033	0.040	0.041	0.031	0.039	0.037
	1.25 dB	*SNR*	22.97	23.94	23.57	21.82	18.76	23.57	19.79	19.07	23.55	22.54	21.96
		RMSE	0.029	0.033	0.033	0.033	0.042	0.033	0.037	0.038	0.030	0.038	0.035
	5 dB	*SNR*	23.45	24.66	23.65	23.08	20.81	23.66	20.69	21.01	24.00	22.81	22.78
		RMSE	0.027	0.030	0.033	0.030	0.035	0.030	0.034	0.030	0.028	0.037	0.031

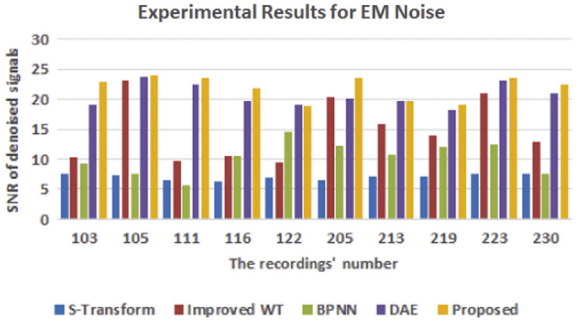

Fig. 8. De-noised SNR for the EM noise case with 1.25 dB.

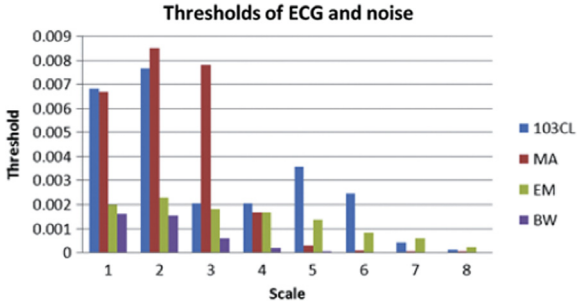

Fig. 10. Thresholds of ECG and noise with *SNR*=5 dB.

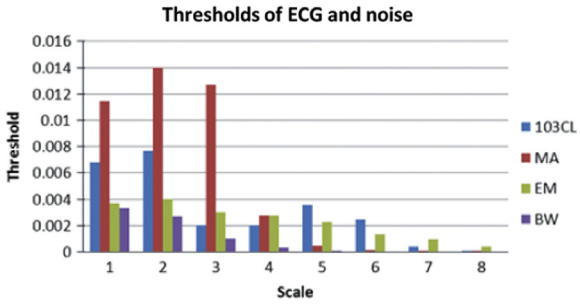

Fig. 9. Thresholds of ECG and noise with *SNR*=1.25 dB.

23.74 dB, respectively, compared with the proposed method SNR of 24.41 dB. The RMSEs for this recording were 0.225, 0.063, 0.145, 0.029, and 0.027, respectively.

Table 2 illustrates the RMSE and SNR of the MA noise enhanced signals using the S-Transform, improved WT, BPNN, DAE and the proposed method. The SNR for each recording after denoising for the MA noise case are shown in Fig. 7. The S-Transform, BPNN and the WT methods provided a minor improvement in the RMSE and SNR, and the DAE method provided further enhancement. The proposed method showed further improvement over the DAE method. For example, the results for recording number 122 showed that for a 1.25 dB input SNR, the S-Transform, WT, BPNN, and DAE outputs had a SNR of 9.67 dB, 7.43 dB, 15.69 dB, and 18.90 dB, respectively, compared with the proposed method SNR of 20.02 dB. The RMSEs for this recording were 0.328, 0.167, 0.151, 0.042, and 0.038, respectively.

Table 3 illustrates the RMSE and SNR of the MA noise enhanced signals using the S-Transform, improved WT, BPNN, DAE and the proposed method. The SNR for each recording after denoising for the EM noise case are shown Fig. 8. The S-Transform, BPNN and the WT methods provided a minor improvement in the RMSE and SNR, and the DAE method provided further enhancement. However, the proposed method showed further improvement over the DAE method. For example, the results for recording number 122

showed that for a 1.25 dB input SNR, the S-Transform, WT, BPNN and DAE outputs had a SNR of 9.67 dB, 7.43 dB, 14.70 dB and 18.90 dB, respectively, compared the proposed method SNR of 20.02 dB. The RMSEs for this recording were 0.328, 0.167, 0.168, 0.042, and 0.038, respectively.

3.3. Discussion

Experimental results for the removal of MA and EM noise indicated that the proposed method provided an improvement over the other methods. However, experimental results for the removal of BW noise indicated little advantage with the proposed method compared with the WT method, though some improvement over the other methods was observed. The WT with scale adaptive thresholding method could filter most of the noise, which is separated from the ECG signal to some degree after wavelet decomposition when the wavelet coefficient of the noise signal was lower than the set threshold. The set threshold for the ECG signal of 103th recording, BW noise, EM noise, and MA noise are shown in Figs. 9 and 10. The BW noise set threshold was much lower than the ECG signal for each scale. However, the EM noise and MA noise set threshold was greater than the ECG signal for some scales. According to Eq. (2), most noise is removed after reconstructing the wavelet coefficients. The residual noise, which is often complex with an unknown distribution in the frequency domain, is subsequently removed by the DNN based improved DAE.

4. Conclusions

We have proposed a novel method of denoising ECG signals containing noise from baseline wander, electrode contact noises, and motion artifacts. This study extends the use of DAE methods by combining it with WT with soft thresholding method. Separately, the DAE method is sufficient for denoising signals contaminated with electrode contact noise and motion artifacts, but less so for removing baseline wander owing to limited notes within the layers. We solve this problem by supplementing the utilized DAE with a WT method. The architecture and calculation of the improved DAE have been presented, and a DNN using the proposed method on various sources of ECG noise has been established.

Experimental results demonstrated that the proposed method improves the expression of ECG signals through multi-level feature extraction. The proposed algorithm was tested on noisy ECG signals computed from the MIT-BIH Arrhythmia and MIT-BIH Noise Stress Test databases. Results showed that the proposed method outperforms the conventional algorithms such as S-Transform, with improvement in the SNR and RMSE.

The major advantages of the proposed method are summarised below:

(1) Complex residual noised, which often has an unknown distribution in the frequency domain, cannot be easily removed by conventional frequency-based noise reduction methods such as the S-Transform method. Our method removes the residual noises by extracting the main characteristics of the ECG signals and reconstructing the clean ECG signals. The training process also helps to improve the performance of the proposed method.
(2) The WT helps to achieve noise reduction in ECG signal processing and also to reduce the number of training samples by reducing the noise characteristics of the samples.
(3) The DNN could represent the ECG signals as a distributed representation, thereby obtaining its essential characteristics. The proposed method takes advantage of a big dataset to improve denoising of the signal, and also be helpful in capturing the main features of ECG signals.

Nonetheless, there are some limitations with the proposed method. Since the learning of the DNN is based on training samples, the key features of the training samples must be comprehensive and carefully selected, representing an average value. The ECG signals contained in the database are actual clinical results with a centrally-distributed feature set owing to the small sample size. After the DNN is trained with the samples from the database, it is not sensitive to some features owing to the small sample size. Future work includes the development of a method to compensate for this unbalanced sample.

Acknowledgments

This work is partially supported by the grants of the Natural Science Foundation of Hebei Province (F2015201112), the Funds for Distinguished Young Scientists of Hebei Province (F2016201186) and the Colleges and Universities in Hebei Province Science and Technology Research Point Project (ZD2015067).

References

Awal, M.A., Ahmad, M., Daut, I., et al., 2012. Wavelet based distortion measurement and enhancement of ECG signal. In: International Conference on Biomedical Engineering (ICoBE), Penang, Malaysia, IEEE, 2012, pp. 373–378.
Awal, M.A., Mostafa, S.S., Ahmad, M., et al., 2014. An adaptive level dependent wavelet thresholding for ECG denoising. Biocybern. Biomed. Eng. 34 (4), 238–249.
Clifford, G.D., Azuaje, F., McSharry, P.E., 2006. Advanced Methods and Tools for ECG Data Analysis. Artech House, Norwood, MA, pp. 55–70.
Dahl, G.E., Yu, D., Deng, L., Acero, A., 2012. Context-dependent pretrained deep neural networks for large-vocabulary speech recognition. IEEE Trans. Audio Speech Lang. Process 20 (1), 30–42.
Erhan, D., Szegedy, C., Toshev, A., et al., 2014. Scalable object detection using deep neural networks. In: 2014 IEEE Conference on Computer Vision and Pattern Recognition (CVPR), Columbus, USA, IEEE, pp. 2155–2162.
Gokhale, P.S., 2012. ECG signal de-noising using discrete wavelet transform for removal of 50 Hz PLI noise. Int. J. Emerg. Technol. Adv. Eng. 2 (5), 81–85.
Kabir, M.A., Shahnaz, C., 2012. Denoising of ECG signals based on noise reduction algorithms in EMD and wavelet domains. Biomed. Signal Process. Control 7 (5), 481–489.
Karagiannis, A., Constantinou, P., 2011. Noise-assisted data processing with empirical mode decomposition in biomedical signals. IEEE Trans. Inf. Technol. Biomed. 15 (1), 11–18.
Moody, G.B., Mark, R.G., 2001. The impact of the MIT-BIH Arrhythmia Database. IEEE Eng. Med. Biol. 20 (3), 45–50.
Moody, G.B., Muldrow, W.E., Mark, R.G., 1984. A noise stress test for arrhythmia detectors. Comput. Cardiol. 11, 381–384.
Moradi, M.H., Ashoori, R.M., Baghbani, K.R., 2014. ECG signal enhancement using adaptive Kalman filter and signal averaging. Int. J. Cardiol. 173 (3), 553–555.
Rahman, M.Z.U., Shaik, R.A., Reddy, D.V.R.K., 2011. Efficient sign based normalized adaptive filtering techniques for cancellation of artifacts in ecg signals: application to wireless biotelemetry. Signal Process. 91 (2), 225–239.
Rahman, M.Z.U., Shaik, R.A., Reddy, D.V., Rama, K., 2012. Efficient and simplified adaptive noise cancelers for ecg sensor based remote health monitoring. IEEE Sens. J. 12 (3), 566–573.
Reddy, G.U., Muralidhar, M., Varadarajan, S., 2009. ECG denoising using improved thresholding based on wavelet transforms. Int. J. Comput. Sci. Netw. Secur. 9, 221–225.
Rodrigues, R., Couto, P. A neural network approach to ECG denoising, Cs.CE, 2012, pp. 1–15.
Sajjad, G.M.S., Rahman, H., Dey, A.K., Biswas, A.M., Islam, Z., Hoque, A.K.M.J., 2012. Performance comparison of modified lms and rls algorithms in denoising of ecg signals. Int. J. Eng. Technol. 2, 466–468.
Sameni, R., Shamsollahi, M.B., Jutten, C., Clifford, G.D., 2007. A nonlinear bayesian filtering framework for ecg denoising. IEEE Trans. Biomed. Eng. 54, 2172–2185.
Samit, A., Manab, K.D., Anil, C., 2013. ECG signal enhancement using S-transform. Comput. Biol. Med. 43 (6), 649–660.
Smital, L., Vitek, M., Kozumplik, J., Provaznik, I., 2013. Adaptive wavelet wiener filtering of ECG signals. IEEE Trans. Biomed. 60 (2), 437–445.
Swietojanski, P., Ghoshal, A., Renals, S., 2014. Convolutional neural networks for distant speech recognition. IEEE Signal Process. Soc. 21 (9), 1120–1124.

Tajane, Kapil, Pitale, Rahul, Umale, Jayant, 2014. Review paper: comparative analysis of mother wavelet functions with the ecg signals. J. Eng. Res. Appl. 4 (1), 38–41.

Vincent, P., Laochelle, H., Bengiol, Y., 2008. Extracting and composing robust features with denoising auto-encoders. In: Proceedings of the 25th International Conference on Machine Learning.

Vincent, P., 2011. A connection between score matching and denoising auto-encoders. Neural Comput. 23 (7), 1661–1674.

Vullings, R., De Vries, B., Bergmans, J.W.M., 2011. An adaptive Kalman filter for ECG signal enhancement. IEEE Trans. Biomed. Eng. 58 (4), 1094–1103.

Xiaopeng, L., Chen, L.Z., 2014. Research on the application of bp neural networks in 3d reconstruction noise filter. Adv. Mater. Res. 998–999, 911–914.